ARTICLES
PUBLISHED ONLINE: 27 MARCH 2011 | DOI: 10.1038/NPHYS1953
nature physics

Direct observation of the full transition from ballistic to diffusive Brownian motion in a liquid

Rongxin Huang[1], Isaac Chavez[1], Katja M. Taute[1], Branimir Lukić[2], Sylvia Jeney[2], Mark G. Raizen[1] and Ernst-Ludwig Florin[1]*

At timescales once deemed immeasurably small by Einstein, the random movement of Brownian particles in a liquid is expected to be replaced by ballistic motion. So far, an experimental verification of this prediction has been out of reach due to a lack of instrumentation fast and precise enough to capture this motion. Here we report the observation of the Brownian motion of a single particle in an optical trap with 75 MHz bandwidth and sub-ångström spatial precision and the determination of the particle's velocity autocorrelation function. Our observation is the first measurement of ballistic Brownian motion of a particle in a liquid. The data are in excellent agreement with theoretical predictions taking into account the inertia of the particle and hydrodynamic memory effects.

Almost 200 years ago, the botanist Robert Brown was the first to systematically investigate the erratic motion of suspended microscopic particles[1]. Under Brown's microscope, each step seemed completely independent of the previous. It is this randomness that is the hallmark of Brownian motion. The origin of the random motion was first successfully explained by Einstein as the amplification of the statistical fluctuations of the surrounding fluid molecules[2]. Since then, the theory of Brownian motion has found broad application in the description of phenomena in many fields in science[3] and even in financial models[4]. A universal description of the cumulative effect of many small, independent, stochastic changes is the common thread that connects this wide range of phenomena.

Due to the fractal nature of a diffusive Brownian particle's trajectory, the length of the path travelled in a given time interval is unknown. Therefore, the particle's velocity is ill-defined, which led to confusion in early attempts to connect the particle's apparent velocity to the temperature as demanded by the equipartition theorem[5]. The mean square displacement (MSD), on the other hand, can be measured and was shown by Einstein to increase linearly with time t: $\mathrm{MSD}(t) = 2Dt$, where D is the particle's diffusion constant.

Deviations from diffusion

Einstein was aware, however, that his stochastic description of the interactions of the particle with the surrounding fluid must break down at short timescales, where the particle's inertia becomes significant[6]. In the inertia-dominated regime, termed ballistic, the particle's motion is highly correlated and therefore allows for the definition of a velocity. Loosely speaking, after receiving an impulse from the surrounding fluid molecules, the particle flies in a straight line with constant velocity before collisions with fluid molecules slow it down and randomize its motion. The first mathematical description of a Brownian particle's dynamics that included its inertia and was applicable over the entire time domain was provided by Langevin[7]. The result is an exponentially damped velocity autocorrelation function (VACF) with a characteristic timescale $\tau_p = m/\gamma$, where m is the mass of the spherical particle and γ is the Stokes viscous drag coefficient. Correspondingly, the MSD approaches $(k_B T/m)t^2$ in the ballistic regime below τ_p, and becomes $2Dt$ at larger times. Here k_B is the Boltzmann constant and T is the temperature.

Hard-sphere simulations[8–11] as well as experiments[12,13], however, showed that, even for timescales much larger than τ_p, Einstein's description already fails. These deviations from random diffusive behaviour were shown to originate from the inertia of the surrounding fluid, which leads to long-lived vortices caused by and in turn affecting the particle's motion. These hydrodynamic memory effects were first described by Vladimirsky[14] and later brought to wider attention by Hinch[15]. Instead of an exponential decay, the VACF shows a long-time tail proportional to $t^{-3/2}$. Correspondingly, the hydrodynamic memory effects introduce an intermediate regime between the purely ballistic t^2 and the diffusive $2Dt$ scaling, where the MSD takes on a rather complicated form[15]. A characteristic timescale for the onset of this effect is given by $\tau_f = r^2\rho_f/\eta$, where r is the particle's radius and ρ_f refers to the density of the fluid and η to its viscosity. The characteristic timescales τ_f and τ_p are related by $\tau_f/\tau_p = 9\rho_f/2\rho_p$, where ρ_p is the particle's density, and hence are generally of the same order of magnitude for the movement of a solid sphere in a liquid. In addition, the correct hydrodynamic treatment modifies the MSD in the ballistic regime to $(k_B T/m^*)t^2$, where m^* is an effective mass given by the sum of the mass of the particle and half the mass of the displaced fluid.

Experimental challenges

In a 1907 paper[16], Einstein declared that, due to the rapid deceleration caused by the viscosity of the medium, it would be impossible to measure the instantaneous velocity of an ultramicroscopic Brownian particle moving in a liquid. In a gas phase, however, the viscosity is more than 50 times lower and hence the timescales of inertial movement are increased accordingly. For microscopic particles in a rarified gas, Blum *et al.*[17] were able to observe the transition from diffusive to ballistic motion by means of video microscopy, and more recently, Li *et al.*[18] verified that their instantaneous velocities follow the Maxwell distribution. In both

[1]Center for Nonlinear Dynamics, The University of Texas at Austin, Austin, Texas 78712, USA, [2]Institut de Physique de la Matière Complexe, Ecole Polytechnique Fédérale de Lausanne (EPFL), CH-1015 Lausanne, Switzerland. *e-mail: florin@chaos.utexas.edu.

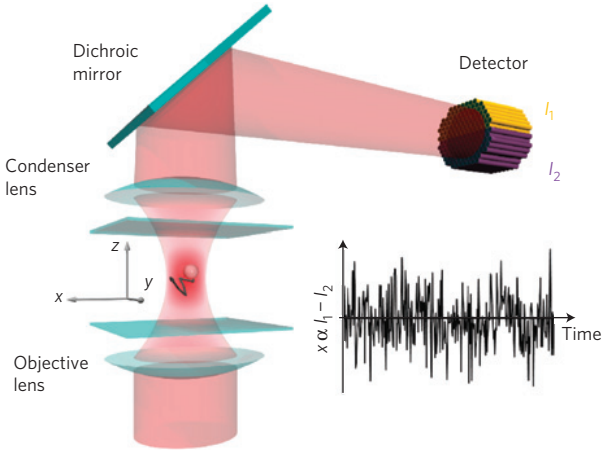

Figure 1 | Schematic diagram of the experiment. A single micrometre-size particle in water is undergoing Brownian motion in the observation volume given by an optical trap. The light scattered by the particle interferes with the unscattered laser light, giving rise to intensity shifts in the back-focal plane of the condenser lens[20,29,30]. Two sets of fibres (here shown in yellow and purple) guide the light to the two photodiodes of a fast, balanced detector. The difference between the intensity signals from the two sets of fibres (I_1 and I_2) is proportional to the particle's position in the x direction.

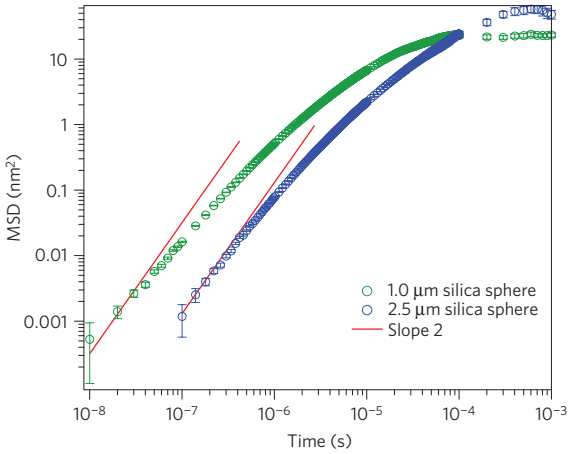

Figure 2 | Example MSD for silica particles 1 μm and 2.5 μm in diameter. The position data were recorded at 100 MHz for 40 ms. The noise floor given by the signal measured in the absence of a particle was subtracted from the MSD. As standard deviations underestimate errors for finite time series with correlations, we estimate the true statistical errors using the 'blocking method'[34]. The red lines show the behaviour expected for ballistic Brownian motion. Because τ_p scales with r^2, the larger bead displays ballistic motion at larger timescales.

cases, the solution to the Langevin equation[19] was fully sufficient to describe the experimental results. In contrast, Brownian motion in a liquid is characterized not only by much faster timescales but also by the added complexity of the rich interplay between the particle and the medium. It is this interplay that enables Brownian particles to act as probes of their environment, an endeavour hitherto hampered by the lack of a validated theory for the interpretation of results.

So far, experiments have only been able to access the non-diffusive regime caused by hydrodynamic memory effects[20,21] and have especially addressed hydrodynamic interactions between neighbouring particles[22–26]. Ballistic Brownian motion of a particle in a liquid, however, has been inaccessible to experiments and hence hydrodynamic theories for this regime have never been verified. The main challenge in the direct observation of the ballistic Brownian motion of a single particle lies in the coupling between length scales and timescales. According to the Stokes–Einstein formula, $D = k_B T/\gamma$, a 1 μm silica bead in water, for instance, will on average move about 1 nm within 1 μs. Purely ballistic Brownian motion is expected on timescales significantly faster than τ_p, which is about 100 ns for the above particle. The corresponding average displacement is of the order of 1 Å. Therefore, resolving ballistic Brownian motion in a liquid requires a position detector with not only extraordinary spatial resolution but, simultaneously, extraordinary temporal resolution. Although progress has been made in achieving higher spatial resolution[27], temporal resolution is still lacking and, so far, no instrument has met both requirements simultaneously. Here we exploit recent improvements in position detector technology for optically trapped particles[28] to for the first time validate hydrodynamic theories for the ballistic regime of Brownian motion for a single particle in a liquid.

Detecting ballistic Brownian motion

A schematic representation of our experimental set-up is shown in Fig. 1. A single particle in water is confined by a harmonic optical trap and undergoes Brownian motion inside the trapping volume. Using laser interferometry[20,29,30], its position–time trace in one lateral dimension is recorded with a high-bandwidth detector system[28]. The confinement by the trap's harmonic potential introduces another timescale $\tau_K = \gamma/K$, where K is the stiffness of the optical trapping potential. For timescales much shorter than τ_K, the motion can be considered free. In the experiments described here, τ_K is typically two orders of magnitude larger than τ_f. This system corresponds to that of a Brownian particle in a harmonic potential as discussed in detail by Clercx and Schram[31] in an extension of Hinch's work[15].

To determine whether we have access to the ballistic motion regime, we compute MSDs from the recorded position–time traces. Figure 2 shows an example of an MSD for a 1 μm silica particle calculated over five orders of magnitude in timescales from about 10 ns to 1 ms. The MSD initially increases, and then reaches a plateau around 0.1 ms. The plateau is caused by the confinement due to the optical trap. For shorter times the particle undergoes free, but not necessarily random Brownian motion. As demonstrated by the error bars, the limit of our temporal resolution is reached by ∼10 ns in the case of a 1 μm silica particle. At this temporal resolution, we can resolve a MSD as small as ∼0.0005 nm², corresponding to ∼20 pm spatial resolution—smaller than the size of a hydrogen atom. The temporal resolution varies for different kinds of particle but is always smaller than τ_p in the experiments presented here. The effect of the particle's inertia on Brownian motion is therefore expected to be visible, and indeed the data for short timescales closely follow the $(k_B T/m^*)t^2$ prediction for ballistic motion.

Whereas both diffusive motion and hydrodynamic memory effect depend only on the size of the particle, and not on its composition, ballistic motion depends on the particle mass. Deviations in behaviour between particles of the same size but different densities hence clearly indicate the presence of particle inertia effects. Figure 3a shows the normalized MSD for 2.5 μm silica and polystyrene particles. The MSD has been normalized to the behaviour expected for the diffusive regime, $2Dt$, and the time axis has been normalized to $\tau_f \approx 1.6$ μs. The fact that the normalized MSD of both particles deviates from unity implies that their motion is not purely diffusive at the timescales shown. At times above ∼2 τ_f the two curves overlap, indicating that the motion in this temporal regime is completely dominated by the fluid inertia. A difference in the MSD values is discernible right around τ_f, and becomes manifest at shorter timescales. The digression is a consequence of the particles' different densities and hence a clear indicator of

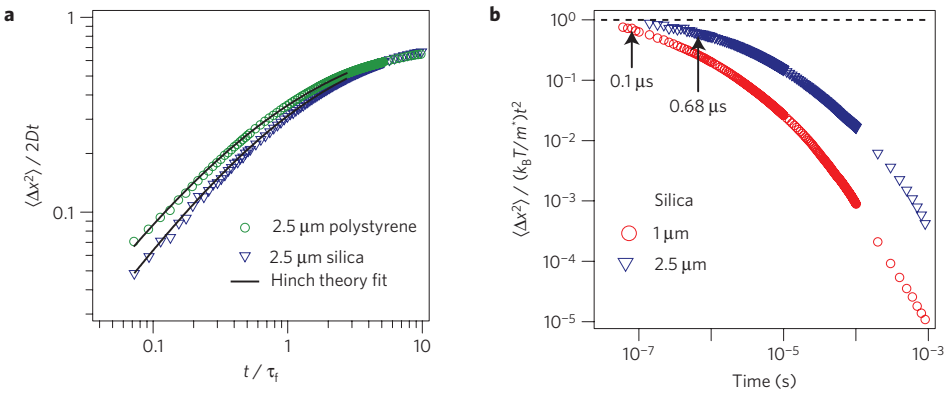

Figure 3 | Ballistic regime. a, Normalized MSD for 2.5 μm silica (1.96 g ml^{-1}) and polystyrene (1.05 g ml^{-1}) particles. The timescale is normalized to τ_f, and the MSD is normalized to the value in the free-diffusion regime $2Dt$. Note that τ_f is the same for both particles. **b**, MSD of 1 and 2.5 μm silica particles normalized to the value in the ballistic regime $(k_BT/m^*)t^2$. Arrows indicate the value of τ_p for each particle.

ballistic motion: silica has a higher density than polystyrene, and so will move more slowly after receiving an impulse from the surrounding water molecules. At the resolution limit of 0.07 τ_f, the two curves differ by a factor of ∼2. As evidenced by both the t^2 scaling of the MSD in Fig. 2 and the density-dependent deviations for same-sized particles in Fig. 3a, our experiments clearly resolve the regime of ballistic motion where the particle's motion is dominated by its own inertia.

Velocity autocorrelation function

To further investigate how closely the particles' behaviour approaches the purely ballistic regime, we normalize the MSD to $(k_BT/m^*)t^2$ for two silica particles with different sizes. Figure 3b shows that the normalized MSD approaches unity for both particles, as expected for purely ballistic motion. The normalized value reaches a maximum of 90% for the larger particle, indicating that the particle maintains a constant velocity after receiving an impulse. Thus, the particle's path is now smooth rather than fractal and the velocity can be determined directly from position measurements. Therefore, for the first time, we are able to compute an experimental VACF of a Brownian particle in a liquid.

Being a derivative, however, the velocities are subject to more noise than positions and hence are more challenging to measure. Particle size and material have to be carefully chosen to maximize the position signal and temporal resolution. The particle's mass needs to be as large as possible to increase τ_p and secure best possible access to the ballistic regime. At the same time, the strength of the position signal depends on both size and particle composition. Due to their well-defined shape and high refractive index ($n = 1.68$), resin particles with a diameter of 2 μm provide a satisfying solution to these requirements. To further reduce the noise, we compute the VACF as an average of 100 separate time traces smoothed to the expected temporal resolution.

Figure 4 shows our experimental results overlaid with a fit of the theoretical expression from the Clercx-and-Schram theory. As the stiffness of the optical trap can be determined by an independent measurement based on position histograms, the only free parameters in the VACF fit are the particle radius and a calibration factor for the position detection. The remarkable agreement between theory and data confirms not only that we are indeed measuring motion in a regime with a well-defined velocity but also that we achieve sufficient resolution and sampling to resolve the characteristic features of the VACF. Even the tiny anti-correlation between 10 μs and 300 μs, caused by reversal of direction at the other side of the optical trap, is faithfully represented by our data.

It should however be noted that, although our spatial resolution is sufficient to clearly resolve ballistic features of the MSD and even

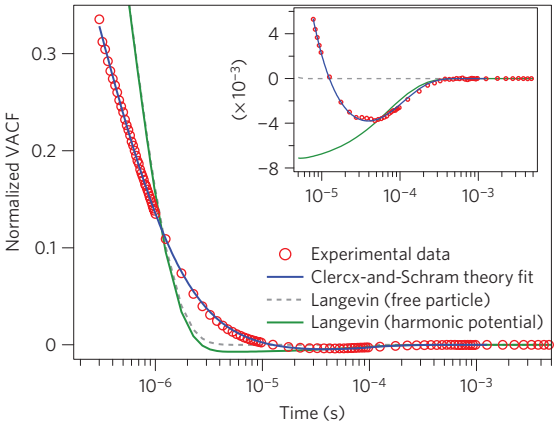

Figure 4 | Experimental VACF and theoretical description. The VACF normalized to k_BT/m^* is shown for a 2 μm resin particle in an optical trap with force constant 280 pN μm^{-1}. The data are averages over 100 segments sampled at 50 MHz for 80 ms. Above 1 μs, the data were averaged to 20 points per decade for fitting and display. The blue line shows the Clercx-and-Schram theory fit to the whole experimental VACF. The fit includes a calibration factor as the only fitting parameter. The grey and green lines show the solution to the Langevin equation for the same particle in the absence and presence of the harmonic trap, respectively. These two lines are normalized to their limit k_BT/m. Because they neglect hydrodynamic memory effects, these curves sharply deviate from the data at short timescales. For times shorter than $\tau_f = 1$ μs, the velocity correlations are weaker than expected from the Langevin equation due to the inertia of the fluid, while at larger times the correlations are stronger because the particle is carried along by the inertia of the fluid.

compute a VACF, both quantities are averages over large data sets. Only with drastic further improvements in spatial resolution will it be possible to measure position–time traces that are smooth enough to allow for the determination of the instantaneous velocity of a Brownian particle in a liquid. In principle, such a measurement should return the Maxwell velocity distribution in accordance with the equipartition theorem.

Particle–liquid interactions at short timescales

Care needs to be taken here to correctly account for the particle's fluid envelope, which increases its effective mass to m^*. The equipartition theorem demands that $m\langle v^2\rangle = k_BT$, where v is the particle's velocity. The VACF expressions derived by Clercx and Hinch, however, give a limit of $\langle v^2\rangle = k_BT/m^*$ for short times. This apparent conflict was discussed by Vladimirsky and Terletzky[14] as

well as Giterman and Gertsenshtein[32], who pointed out the effects of the non-negligible compressibility of the fluid at short timescales. The hydrodynamic treatment that increases the particle's effective mass to m^* assumes the fluid to be incompressible. However, on timescales of the order of $\tau_c = r/c$, where c is the speed of sound in the fluid, the particle interacts elastically with the surrounding fluid—that is, the fluid is compressible. Only on timescales shorter than τ_c will the particle be able to decouple from its fluid envelope, and the velocity variance will approach $\langle v^2 \rangle = k_B T/m$ as demanded by the equipartition theorem. The decrease in the VACF from $k_B T/m$ to $k_B T/m^*$ was shown by Zwanzig and Bixon[33] to take the form of exponentially damped oscillations.

An experimental verification of the oscillatory short-time decay of the VACF is currently out of reach for a single particle in a liquid. For a 1 μm silica bead in water, $\tau_c \approx 0.3$ ns and the corresponding displacement is about 1 pm. Significant improvements in detector technology are required to gain access to this regime. Nevertheless, a valid single-particle theory from the diffusive to the ballistic regime is of utmost importance for the correct description of multiple-particle phenomena such as the viscoelastic properties of colloidal suspension. In addition, the newly gained ability to measure fast Brownian motion of an individual particle paves the way for detailed studies of confined Brownian motion and Brownian motion in heterogeneous media.

Methods

Experimental set-up. Samples were prepared as dilute solutions in purified water (Milli-Q, Millipore) with a typical number density of one particle per $200 \times 200 \times 200\,\mu m^3$ volume to avoid hydrodynamic interactions between particles. The particles used in the experiments are commercially available glass and polystyrene beads (SS03N, SS05N and PS05N, Bangs Laboratories) and melamine resin beads (90637, Sigma-Aldrich). Particles were trapped in the focus of a 1,064 nm laser with a power of 600 mW. Experiments were carried out at 296 ± 1 K after sufficient time for the set-up and sample to attain thermal equilibrium. The distance between the trapped particle and the bottom coverslip was at least 10 times the particle's diameter, ensuring that hydrodynamic interactions between the particle and the bottom coverslip are negligible. High-speed position detection in one lateral direction is possible with an array of fibres that guide the light to a fast, balanced photodetector. The use of the fibre bundle as an intermediate unites the optical requirement of large collection area with the small photodiodes required for fast measurements. A detailed description of the detector can be found in ref. 28. The detector output (75 MHz bandwidth) is recorded with a high-bandwidth digitizer at 100 MHz and 14 bits for 40 ms. The length of the data segment is limited by the size of the digitizer's on-board memory.

For the VACF experiments, 100 position traces were recorded at 50 MHz for 40 ms each and subsequently smoothed to a resolution of 5 MHz to decrease contributions from electronic noise. The VACF was computed as an average over the 100 time traces.

Calibration and data fitting. To obtain the calibration for the position signal from our detector, the MSD at times much shorter than τ_K is fitted to the expression derived by Hinch[15] for free Brownian motion including inertia effects due to both the fluid and the particle. Input parameters for the fits are $\rho_f = 1\,g\,ml^{-1}$ and $\eta = 10^{-3}$ Pa s as well as the densities $1.96\,g\,ml^{-1}$, $1.05\,g\,ml^{-1}$ and $1.5\,g\,ml^{-1}$ for silica, polystyrene and resin particles, respectively. The only free parameters in the fits are the particle radius and the multiplicative calibration factor. For the VACF, the particle radius is obtained analogously. As the stiffness of the trap can be determined independently from the width of the position distribution obtained from a 10 s time series sampled at 50 kHz, this leaves the calibration factor as the only free parameter for the fit of the full VACF.

Although it is in principle possible to fit the entire time domain using complementary expressions for both MSD and VACF derived by Clercx[31] that are corrected for the presence of a harmonic potential, focusing on the time regime independent of the trap yields more precise results because of the smaller number of fit parameters involved.

Temporal and spatial resolution. The main sources of noise in our experiments are laser and electronic noise. This noise is uncorrelated to the motion of the particle and leads only to an offset in the measured MSD. The offset was determined by measurements in the absence of a particle in the trap and was subtracted from the MSD measured with a particle in the trap.

The nominal bandwidth of our detector is only 75 MHz; however, we obtain reasonable data even at a sampling frequency of 100 MHz (Fig. 2). The reason for this may lie in the fact that the nominal bandwidth is generally specified for large signals while the signals we are looking at on fast timescales are extremely small.

Received 29 April 2010; accepted 15 February 2011; published online 27 March 2011

References

1. Brown, R. A brief account of microscopical observations made in the months of June, July and August, 1827 on the particles contained in the pollen of plants; and on the general existence of active molecules in organic and inorganic bodies. *Phil. Mag.* **4,** 161–173 (1828).
2. Einstein, A. Über die von der molekularkinetischen Theorie der Wärme geforderte Bewegung von in ruhenden Flüssigkeiten suspendierten Teilchen. *Ann. Phys.* **322,** 549–560 (1905).
3. Frey, E. & Kroy, K. Brownian motion: A paradigm of soft matter and biological physics. *Ann. Phys.* **14,** 20–50 (2005).
4. Black, F. & Scholes, M. S. The pricing of options and corporate liabilities. *J. Political Econ.* **81,** 637–654 (1973).
5. Smoluchowski, M. Zur kinetischen Theorie der Brownschen Molekularbewegung und der Suspensionen. *Ann. Phys.* **21,** 756–780 (1906).
6. Einstein, A. Zur Theorie der Brownschen Bewegung. *Ann. Phys.* **324,** 371–381 (1906).
7. Langevin, P. Sur la théorie du mouvement brownien. *C.R. Acad. Sci. Paris* **146,** 530–533 (1908).
8. Rahman, A. Correlations in the motion of atoms in liquid argon. *Phys. Rev.* **136,** A404–A411 (1964).
9. Rahman, A. Liquid structure and self-diffusion. *J. Chem. Phys.* **45,** 2585–2592 (1964).
10. Alder, B. J. & Wainwright, T. E. Velocity autocorrelations for hard spheres. *Phys. Rev. Lett.* **18,** 988–990 (1967).
11. Alder, B. J. & Wainwright, T. E. Decay of the velocity autocorrelation function. *Phys. Rev. A* **1,** 18–21 (1970).
12. Paul, G. L. & Pusey, P. N. Observation of a long-time tail in Brownian motion. *J. Phys. A.* **14,** 3301–3327 (1981).
13. Weitz, D. A., Pine, D. J., Pusey, P. N. & Tough, R. J. A. Nondiffusive Brownian motion studied by diffusing-wave spectroscopy. *Phys. Rev. Lett.* **63,** 1747–1750 (1989).
14. Vladimirsky, V. & Terletzky, Y. A. Hydrodynamical theory of translational Brownian motion. *Zh. Eksp. Teor. Fiz.* **15,** 258–263 (1945).
15. Hinch, E. J. Application of the Langevin equation to fluid suspensions. *J. Fluid Mech.* **72,** 499–511 (1975).
16. Einstein, A. Theoretische Bemerkungen über die Brownsche Bewegung. *Z. Elektrochem.* **13,** 41–42 (1907).
17. Blum, J. *et al.* Measurement of the translational and rotational Brownian motion of individual particles in a rarefied gas. *Phys. Rev. Lett.* **97,** 230601 (2006).
18. Li, T., Kheifets, S., Medellin, D. & Raizen, M. G. Measurement of the instantaneous velocity of a Brownian particle. *Science* **328,** 1673–1675 (2010).
19. Uhlenbeck, G. E. & Ornstein, L. S. On the theory of Brownian motion. *Phys. Rev.* **36,** 823–841 (1930).
20. Lukić, B. *et al.* Direct observation of nondiffusive motion of a Brownian particle. *Phys. Rev. Lett.* **95,** 160601 (2005).
21. Jeney, S., Lukić, B., Kraus, J. A., Franosch, T. & Forró, L. Anisotropic memory effects in colloidal diffusion. *Phys. Rev. Lett.* **100,** 240604 (2008).
22. Zhu, J. X., Durian, D. J., Muller, J., Weitz, D. A. & Pine, D. J. Scaling of transient hydrodynamic interactions in concentrated suspensions. *Phys. Rev. Lett.* **68,** 2559–2562 (1992).
23. Kao, M. H., Yodh, A. G. & Pine, D. J. Observation of Brownian-motion on the timescale of hydrodynamic interactions. *Phys. Rev. Lett.* **70,** 242–245 (1993).
24. Henderson, S., Mitchell, S. & Bartlett, P. Propagation of hydrodynamic interactions in colloidal suspensions. *Phys. Rev. Lett.* **88,** 088302 (2002).
25. Liverpool, T. B. & MacKintosh, F. C. Inertial effects in the response of viscous and viscoelastic fluids. *Phys. Rev. Lett.* **95,** 208303 (2005).
26. Atakhorrami, M., Koenderink, G. H., Schmidt, C. F. & MacKintosh, F. C. Short-time inertial response of viscoelastic fluids: Observation of vortex propagation. *Phys. Rev. Lett.* **95,** 208302 (2005).
27. Neuman, K. C. & Block, S. M. Optical trapping. *Rev. Sci. Instrum.* **75,** 2787–2809 (2004).
28. Chavez, I., Huang, R. X., Henderson, K., Florin, E-L. & Raizen, M. G. Development of a fast position-sensitive laser beam detector. *Rev. Sci. Instrum* **79,** 105104 (2008).
29. Gittes, F. & Schmidt, C. F. Interference model for back-focal-plane displacement detection in optical tweezers. *Opt. Lett.* **23,** 7–9 (1998).
30. Pralle, A., Prummer, M., Florin, E.L., Stelzer, E. H. K. & Horber, J. K. H. Three-dimensional high-resolution particle tracking for optical tweezers by forward scattered light. *Microsc. Res. Tech.* **44,** 378–386 (1999).
31. Clercx, H. J. H. & Schram, P. P. J. M. Brownian particles in shear flow and harmonic potentials: A study of long-time tails. *Phys. Rev. A* **46,** 1942–1950 (1992).

32. Giterman, M. Sh. & Gertsenshtein, M. E. Theory of the Brownian motion and the possibilities of using it for the study of the critical state of a pure substance. *Sov. Phys. JETP* **23** (4), 722–728 (1966).
33. Zwanzig, R. & Bixon, M. Compressibility effects in the hydrodynamic theory of Brownian motion. *J. Fluid. Mech.* **69,** 21–25 (1975).
34. Flyvbjerg, H. & Petersen, H. G. Error estimates on average of correlated data. *J. Chem. Phys.* **91,** 461–466 (1989).

Acknowledgements

This research was supported by NSF grants PHY-0647144 and DBI-0552094. S.J. and B.L. acknowledge support from the NCCR Nanoscale Science. M.G.R. acknowledges support from the Sid W. Richardson Foundation and the R. A. Welch Foundation, grant number F-1258. We thank V. Zyuzin for translating ref. 14.

Author contributions

R.H. and E-L.F. conceived the experiment. B.L. and S.J. contributed to the planning of the early experiments and provided an early version of the VACF analysis software. I.C., R.H., E-L.F. and M.G.R. developed, built and characterized the fast position detector, and incorporated it into the set-up. R.H. carried out the experiments in part assisted by I.C. R.H. analysed the data. R.H., K.M.T. and E-L.F. interpreted the data and wrote the manuscript. All authors discussed and commented on the final version of the manuscript.

Additional information

The authors declare no competing financial interests. Reprints and permissions information is available online at http://npg.nature.com/reprintsandpermissions. Correspondence and requests for materials should be addressed to E-L.F.